Journal of Photochemistry, *38* (1987) 1 - 13

ABSORPTION CROSS-SECTIONS OF CF_2 IN THE $\tilde{A}\ ^1B_1$–$\tilde{X}\ ^1A_1$ TRANSITION AT 0.5 nm INTERVALS AND ABSOLUTE RATE CONSTANT FOR $2CF_2 \rightarrow C_2F_4$ AT 298 ± 3 K

STEVEN SHARPE, BARRY HARTNETT, HARNEET S. SETHI and DHANWANT S. SETHI

CTI Research Corporation and Chemistry Department, University of Bridgeport, Bridgeport, CT 06601 (U.S.A.)

(Received July 24, 1986; in revised form October 6, 1986)

Summary

The absorption cross-sections σ_{CF_2} for the CF_2 radical in the UV for the transition $\tilde{A}\ ^1B_1 \leftarrow \tilde{X}\ ^1A_1$ at 0.5 nm intervals were obtained. CF_2 was produced by the flash photolysis of C_2F_4 and C_3F_6 between 185 and 209 nm. The σ_{CF_2} values determined with the quantum yield ϕ_{CF_2} of CF_2 as 1.0 from the photodissociation of CF_3CFCF_2 and $\phi_{CF_2} = 2.0$ in the photolysis of C_2F_4 were identical within the experimental error of ±15%. HBr actinometry with the emission spectra of the lamps and the σ *vs.* wavelength characteristics of C_2F_4 and C_3F_6 were used to determine the absolute number of photons absorbed per flash. A maximum σ_{CF_2} of $(2.91 \pm 0.44) \times 10^{-17}$ cm^2 molecule^{-1} was obtained at 249.0 nm. This was compared with values reported in the literature. The oscillator strength of the CF_2 transition was determined to be 0.026.

The decay of CF_2 was studied in flashed C_2F_4, C_2F_4 plus added gas, C_3F_6 and C_3F_6 plus added gas mixtures. In all cases CF_2 was found to decay by the second-order reaction $CF_2 + CF_2 \rightarrow C_2F_4$. The rate constant for this dimerization was found to be $(4.26 \pm 0.43) \times 10^{-14}$ cm^3 molecule^{-1} s^{-1}. No evidence for the reaction of CF_2 with C_2F_4 and C_3F_6 to form the next higher perfluorocarbon was observed.

1. Introduction

Difluorocarbene, CF_2, is of interest for several reasons. Its reaction with NO may have implications in the chemistry of the Earth's troposphere [1], where its production from the UV photodissociation of CF_2Cl_2 could occur [2]. CF_2 formation in the IR multiphoton dissociation (IRMPD) of halocarbons such as CF_2Cl_2 [3, 4], C_2F_3Cl [5] and C_3F_6 [6] is a dominant photodissociation channel. In the case of CF_2Cl_2, in both the IRMPD [7] and the UV laser photolysis [8], CF_2 is a product in one of the dissociation channels.

0047-2670/87/$3.50 © Elsevier Sequoia/Printed in The Netherlands

Its yield in such reactions is of interest in enhancing understanding of unimolecular reactions [9]. Its detection as a monitor in fluorocarbon plasmas used for etching semiconductor devices [10] is of considerable practical interest. The temporal variation of CF_2 concentration in such applications is also important in the understanding of gas surface interaction mechanisms. CF_2 is readily formed in discharges used to excite excimer lasers. Because of its strong absorption at 249 nm, this may lead to reduction in laser efficiency in the case of the KrF laser. The identification of CF_2 by photoionization mass spectrometry [11] and the phosphorescence from the $CF_2(^3B_1) \rightarrow CF_2(^1A_1)$ transition [12] in the reaction of $O(^3P)$ with C_2F_4 has been used to bring out important differences between the kinetics of oxygen atom plus fluoroethylene and oxygen atom plus alkene reactions [13]. CF_2 is formed in the disproportionation reaction between fluoroalkyl radicals. The disproportionation–combination ratio in such reactions apparently depends on the nature of the halocarbon radicals [14] and their internal energies. An interesting explanation for this based on Benson's [15] suggestion of assigning a considerably more polar character to the transition state for the disproportion compared with the combination pathway has been proposed by Pritchard *et al.* [16].

In this paper, we report the low resolution absorption spectrum of CF_2 in the $\tilde{A}\ ^1B_1$–$\tilde{X}\ ^1A_1$ band. A direct determination of the rate constant for the dimerization of CF_2 at room temperature was also made. The motivation for this work comes from our interest in (i) the identification of CF_2 produced in semiconductor etching by fluorocarbons and (ii) its quantum yield from the photodissociation of CF_2Cl_2 [2].

The flash photolysis of C_2F_4 and C_3F_6 at wavelengths below 210 nm has been used to generate CF_2 in its ground state $\tilde{X}\ ^1A_1$ [17, 18]. The absorption band for the transition $A\ ^1B_1$–$X\ ^1A_1$ lies between 225 and 270 nm with a maximum around 250 nm [3, 19]. Therefore, a time-resolved UV optical absorption flash photolysis set-up offers a convenient technique for the study of the CF_2 radical.

In this investigation, CF_2 was produced by the flash photolysis of C_2F_4 and C_3F_6.

2. Experimental details

The flash photolysis apparatus was of conventional design. The lamps were made from 10 cm lengths of quartz tubing of 10 mm inside diameter and stainless steel electrodes. The filling mixture consisted of krypton and a trace of oxygen at a total pressure of 25 Torr. Oxygen was used to minimize tail emissions. The lamps were mostly operated at energies between 180 and 200 J, except in order-of-reaction experiments where the range used was between 50 and 288 J. The half-peak-height flash duration was less than 5 μs. Absorption changes (to the base e) of $\pm 8.65 \times 10^{-5}$ cm^{-1} could be measured 50 μs after the initiation of the flash.

A quartz photolysis cell of 10 cm length and 10 mm inside diameter with a quartz optical window at either end was used in most of the work. Some experiments with a quartz cell of 20 mm inside diameter were also conducted to ensure that no complications from surface processes existed.

The transients were monitored by using a collimated beam from a 30 W deuterium lamp. After passage through the 10 cm absorption path length of the cell, the transmitted light was focused onto the entrance slit of a 0.5 m Jarrell Ash monochromator. Most measurements were recorded at a bandwidth of 0.16 nm (slit width, 0.10 mm; dispersion, 1.6 nm mm^{-1}) using an EMI 9635 QB photomultiplier at the exit slit. The signal was amplified, measured against an adjustable bucking voltage, and fed into a Biomation 802 transient recorder. Data acquisition and analysis were performed by interfacing the transient recorder to a microcomputer. The photoelectric measuring system response time was less than 30 ns, well below the resolution of 0.5 μs for the transient recorder.

A mercury-free vacuum system capable of pumpdown to 1×10^{-6} Torr was used for gas handling. All gases were purified by repeated freeze–thaw cycles and volatilized by fractional distillation using appropriate slush baths. Purity checks on gases were performed by mass spectrometry. Pressures were measured by a quartz spiral gauge.

Hydrogen produced in the HBr actinometry [20] was determined by a quadrupole mass spectrometer to establish incident light intensity between 185.0 and 250.0 nm. The wavelength dependence of the emission from the flash lamps was determined by monitoring the scattered light at 1.0 nm intervals with a photodetector. This information was coupled with the HBr actinometry value to arrive at the incident photon flux in the photolysis region 185.0 - 209.0 nm. A typical such value was 1.8×10^{15} photons $flash^{-1}$ cm^{-3}.

The absorption spectra of C_2F_4 and C_3F_6 at various pressures in cells of path lengths 1.0, 5.0, 8.0 and 10.0 cm were recorded on a Cary 17D spectrophotometer.

3. Results and discussion

We define the absorption cross-section σ (cm^2) at a given wavelength by Beer's relation

$$I = I_0 \exp(-\sigma n l) \tag{1}$$

In eqn. (1) I_0 and I are the incident and transmitted intensities respectively, n (molecule cm^{-3}) is the gas concentration and l (cm) is the absorption path length. Plots of $(1/l) \ln(I_0/I)$ *vs.* n at 1.0 nm intervals were used to obtain σ. These values for C_2F_4 and C_3F_6 at a bandwidth of 1.0 nm are given in Table 1. Each value represents the linear least-squares fit slope of at least ten experimental points. In no case was the two-standard deviation error in σ greater than 6.7%. No vibrational structure was observed in the

TABLE 1

Absorption cross-sections $\sigma(\Lambda)$ (cm^2) for C_2F_4 and C_3F_6 at 1.0 nm intervals at room temperature

Λ (nm)	C_2F_4	C_3F_6
185	6.08×10^{-18}	6.34×10^{-18}
186	7.95×10^{-18}	5.88×10^{-18}
187	8.52×10^{-18}	4.86×10^{-18}
188	8.67×10^{-18}	4.12×10^{-18}
189	6.99×10^{-18}	3.22×10^{-18}
190	5.22×10^{-18}	2.54×10^{-18}
191	4.77×10^{-18}	1.98×10^{-18}
192	4.84×10^{-18}	1.45×10^{-18}
193	5.21×10^{-18}	1.12×10^{-18}
194	4.79×10^{-18}	8.40×10^{-19}
195	3.47×10^{-18}	6.12×10^{-19}
196	2.07×10^{-18}	4.41×10^{-19}
197	1.27×10^{-18}	3.26×10^{-19}
198	7.59×10^{-19}	2.42×10^{-19}
199	4.54×10^{-19}	1.66×10^{-19}
200	2.65×10^{-19}	1.20×10^{-19}
201	1.61×10^{-19}	8.59×10^{-20}
202	9.30×10^{-20}	5.97×10^{-20}
203	6.01×10^{-20}	4.44×10^{-20}
204	4.07×10^{-20}	3.10×10^{-20}
205	5.85×10^{-20}	2.39×10^{-20}
206	4.78×10^{-20}	2.57×10^{-20}
207	3.17×10^{-20}	1.66×10^{-20}
208	3.16×10^{-20}	4.17×10^{-21}
209	2.63×10^{-20}	3.39×10^{-21}

spectra of C_2F_4 or C_3F_6 and σ values were independent of the bandwidth down to the lowest attempted limit of 0.01 nm. The average absorption cross-section σ_{av} for the photodissociation range 185.0 - 209.0 nm for both C_2F_4 and C_3F_6 was determined by the graphic integration of the σ *vs.* wavelength plots. The σ_{av} values for C_2F_4 and C_3F_6 were 2.65×10^{-18} cm^2 and 1.18×10^{-18} cm^2 respectively.

3.1. Absorption spectrum of CF_2 in the $\tilde{A}\ ^1B_1$–$\tilde{X}\ ^1A_1$ band

A typical time-resolved transient signal observed at the absorption maximum of 249.0 nm is shown in Fig. 1. The minimum delay time after the flash initiation at which absorption by CF_2 could be measured was about 50 μs. From the kinetic measurements described below (Section 3.2), we estimate that at 50 μs the decrease in CF_2 is well below 1% of its initial concentration. Therefore, it is reasonable to identify the optical density (at 50 μs) with the initial concentration of CF_2. The optical density OD_{max} at this time was used to determine the absorption spectra of CF_2.

In Table 2, we show the results of some experiments on the effect of bandwidth on OD_{max}. For slit widths from 0.025 to 0.125 mm, *i.e.* a

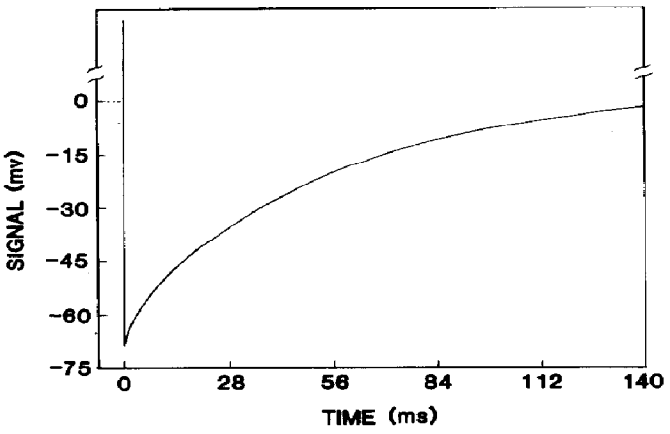

Fig. 1. Time dependence of the transient signal ($P_{C_3F_6}$ = 20.14 Torr; P_{N_2} = 279.4 Torr; flash energy, 200 J; Λ = 249.0 nm; absorption path length, 10 cm; bandpass, 0.16 nm; I_0 = 0.50 V).

TABLE 2

Effect of bandwidth on the initial optical density[a] OD_{max} of CF_2 at 249.0 nm for two representative mixtures

Bandwidth (nm)	*Mixture A*[b]	*Mixture B*[c]	*Average OD*[d]$_{max}$	
			Mixture A	*Mixture B*
0.040	0.160	0.180		
0.080	0.168	0.187		
0.120	0.157	0.184	0.160 ± 0.010	0.182 ± 0.007
0.160	0.162	0.178		
0.200	0.155	0.181		

[a]For definition see eqn. (1). Each value represents an average of at least seven determinations, one per mixture. OD_{max} values are corrected for flash-to-flash intensity variations.
[b]Mixture A, C_3F_6 (20.0 - 20.37 Torr) + N_2 (80.0 ± 1.00 Torr).
[c]Mixture B, C_2F_4 (10.0 ± 0.1 Torr) + N_2 (90.0 ± 1.00 Torr).
[d]The errors quoted are two standard deviations from the mean values.

bandwidth from 0.040 to 0.200 nm, no change in the OD_{max} or in its variation with time was observed. All the data on CF_2 reported in this work were collected at a bandwidth of 0.160 nm. OD_{max} in the entire absorption region 225 - 270 nm was found to be independent of the pressure or the nature of the added gas (nitrogen, argon or SF_6). In initial experiments, the decay kinetics were analyzed at 240.5, 243.0, 245.5, 246.0, 248.5, 249.0, 252.0, 255.5 and 258.5 nm to establish that the absorption in the entire band corresponded to CF_2 alone.

The transient spectra in the photolysis of C_2F_4, C_2F_4 plus added gas, C_3F_6 and C_3F_6 plus added gas were identical with each other in all respects, except that in the case of C_3F_6 and C_3F_6 plus added gas the optical densities were lower.

The OD_{max} *vs.* wavelength data for CF_2 are a measure of its relative absorption cross-sections. To evaluate σ_{CF_2} *vs.* wavelength, it is necessary to know n_{CF_2} in eqn. (1). The concentration of CF_2 produced in the flash photolysis of C_2F_4 or C_3F_6 can be represented by

$$n_{CF_2} = I_i f\{1 - \exp(-\sigma_{av} nl)\}\phi_{CF_2} \tag{2}$$

In eqn. (2) $I_i f$ represents the integrated incident photon intensity corrected for wavelength dependence by the procedure described in Section 2. The remaining terms correspond to the appropriate fluorocarbon. σ_{av} and n have the same significance as in eqn. (1) and ϕ_{CF_2} represents the quantum yield of CF_2 formation. The only unknown in eqn. (2) is ϕ_{CF_2}. Our observation of no structure in the absorption spectra of C_2F_4 and C_3F_6 and the independence of the n_{CF_2} from the pressure and the nature of the added gas up to a total pressure of 800 Torr indicate excitation to a state with a lifetime of less than 10^{-13} s and dissociation on a repulsive potential energy surface within a single vibrational period for both fluorocarbons. Thus, the quantum yield of photodissociation for these two molecules is indeed unity.

The photodissociation of C_2F_4 and C_3F_6 can be represented by the following reactions:

$$C_2F_4 + h\nu \longrightarrow 2CF_2 \tag{3}$$

$$C_3F_6 + h\nu \longrightarrow CF_2 + CFCF_3 \tag{4}$$

$$C_3F_6 + h\nu \longrightarrow CF_3 + CFCF_2 \tag{5}$$

This means that $\phi_{CF_2} = 2$ in eqn. (2) in the photolysis of C_2F_4. In the case of C_3F_6, ϕ_{CF_2} may be between zero and unity, depending on the contribution of reaction (5). The evidence for the absence of any measurable contribution from reaction (5) comes from Dalby's work [18] on the photolysis of C_3F_6 wherein a value of $\phi_{CF_2} = 1.0$ was determined by product analysis measurements. This is supported by the fact that n_{CF_2} determined from our C_3F_6 photolysis experiments with $\phi_{CF_2} = 1$ in eqn. (2) and hence the σ_{CF_2} values are in agreement with the results from the C_2F_4 experiments. For example, the average OD_{max} values in Table 2 with $\phi_{CF_2} = 1$ and $\phi_{CF_2} = 2$ from the photolyses of C_3F_6 and C_2F_4 lead to σ_{CF_2} of 2.94×10^{-17} cm^2 and 2.74×10^{-17} cm^2 respectively at 249.0 nm. The average σ_{CF_2} at 249.0 nm from all the experiments on C_2F_4 and C_3F_6 was $(2.91 \pm 0.44) \times 10^{-17}$ cm^2. The error represents a two-standard deviation confidence limit of at least 95%. When σ_{CF_2} values were averaged separately for C_2F_4 and C_3F_6 experiments, the results were indistinguishable from the above average.

Our σ_{CF_2} at 249.0 nm is in excellent agreement with Tyerman [17], but it is 2.3 times larger than the estimate of Dalby [18]. Dalby observed a CF_2 intensity dependence on the slit width of the spectrograph, indicating perhaps complications from the scattered light. Duperrex and Van den Bergh [3] obtained a σ_{CF_2} of $8.03 \pm 1.4 \times 10^{-18}$ cm^2 at a bandwidth of 2.0 nm at 249.0 nm. We suspect that the above value is too low as a result of the same reason

as in the case of Dalby and perhaps because of the invalidity of Beer's law at 2.0 nm bandwidth.

In Table 3, the σ_{CF_2} *vs.* wavelength data are presented for the entire absorption band for the transition $\tilde{A}\ ^1B_1 - \tilde{X}\ ^1A_1$ at 0.5 nm intervals on the basis of a σ_{CF_2} value of 2.91×10^{-17} cm^2 at 249.0 nm. All the data are based on the combined C_2F_4 and C_3F_6 experiments. The oscillator strength f for the band was derived from Table 3 by using the relation

$$f = 4.32 \times 10^{-9} \int \epsilon_{\bar{\nu}}\, d\bar{\nu} \qquad (6)$$

TABLE 3

Absorption cross-section $\sigma_{CF_2}(\Lambda)$ for CF_2 in the $\tilde{A}\ ^1B_1 \leftarrow \tilde{X}\ ^1A_1$ band at 0.5 nm intervals in the 229.0 - 262.5 nm range at room temperature[a]

Λ (nm)	σ_{CF_2} (cm^2)
229.0	6.69×10^{-19}
229.5	
230.0	
230.5	
231.0	
231.5	5.82×10^{-19}
232.0	
232.5	3.49×10^{-19}
233.0	6.40×10^{-19}
233.5	1.34×10^{-18}
234.0	3.32×10^{-18}
234.5	2.68×10^{-18}
235.0	1.95×10^{-18}
235.5	1.14×10^{-18}
236.0	1.14×10^{-18}
236.5	
237.0	6.29×10^{-18}
237.5	4.31×10^{-18}
238.0	2.12×10^{-18}
238.5	1.75×10^{-18}
239.0	1.89×10^{-18}
239.5	4.05×10^{-18}
240.0	7.07×10^{-18}
240.5	7.71×10^{-18}
241.0	1.98×10^{-18}
241.5	1.98×10^{-18}
242.0	4.37×10^{-18}
242.5	8.76×10^{-18}
243.0	1.39×10^{-17}
243.5	4.77×10^{-18}
244.0	2.65×10^{-18}
244.5	3.41×10^{-18}
245.0	3.93×10^{-18}
245.5	8.18×10^{-18}
246.0	2.46×10^{-17}
246.5	5.53×10^{-18}

TABLE 3 *(continued)*

Λ (nm)	σ_{CF_2} (cm^2)
247.0	2.53×10^{-18}
247.5	3.78×10^{-18}
248.0	6.02×10^{-18}
248.5	9.23×10^{-18}
249.0	2.91×10^{-17}
249.5	8.24×10^{-18}
250.0	1.72×10^{-18}
250.5	3.70×10^{-18}
251.0	3.81×10^{-18}
251.5	8.12×10^{-18}
252.0	2.48×10^{-17}
252.5	4.02×10^{-18}
253.0	2.12×10^{-18}
253.5	1.63×10^{-18}
254.0	1.75×10^{-18}
254.5	4.71×10^{-18}
255.0	7.57×10^{-18}
255.5	1.67×10^{-17}
256.0	
256.5	7.57×10^{-19}
257.0	1.11×10^{-18}
257.5	3.06×10^{-18}
258.0	5.65×10^{-18}
258.5	1.51×10^{17}
259.0	2.24×10^{-18}
259.5	9.60×10^{-19}
260.0	1.46×10^{-18}
260.5	
261.0	
261.5	2.01×10^{-18}
262.0	1.37×10^{-18}
262.5	1.75×10^{-18}

[a]Blanks in the σ_{CF_2} column indicate a value of less than 2.5×10^{-19} cm^2.

In the above equation $\epsilon_{\bar{\nu}}$ ($l\ mol^{-1}\ cm^{-1}$) represents the extinction coefficient at the wavenumber $\bar{\nu}$ (cm^{-1}). The integration limits are the wavenumbers corresponding to 262.5 nm and 229 nm. A value of $f = 0.026$ was obtained. This does not account for any error due to low spectral resolution. This can be compared with a value of 0.028 obtained by Tyerman [17] in a similar determination and an approximate estimate of 0.015 based on a lifetime of 61.0 ns [21] for the $\tilde{A}$ state.

3.2. Kinetics of CF_2 disappearance

The decay of CF_2 formed from the photolysis of C_2F_4 in reaction (3) can be represented by reactions

$$CF_2 + CF_2 \longrightarrow C_2F_4 \qquad (7)$$

$$CF_2 + C_2F_4 \longrightarrow C_3F_6 \quad (8)$$

$$CF_2 + CF_2 + M \longrightarrow C_2F_4 + M \quad (9)$$

$$CF_2 + C_2F_4 + M \longrightarrow C_3F_6 + M \quad (10)$$

M in reactions (9) and (10) is C_2F_4 or the added inert gas.

By conducting mass spectrometric analyses of calibration mixtures of C_3F_6 in large excess of C_2F_4 and added inert gases such as nitrogen, we determined the detection sensitivity for C_3F_6. No C_3F_6 was detected in any experiments even when photolyses mixtures were subjected to as many as 15 - 20 flashes. In similar experiments with calibrated mixtures containing C_3F_6 in amounts ranging from 0.1% to 1.0% of C_2F_4, we were able to recover C_3F_6 in quantitative amounts. Therefore, reactions (8) and (10) are not important under our experimental conditions.

If reaction (7) is the predominant decay mode for CF_2, then a plot of 1/OD *vs.* time should be linear with a slope of $2k_7/\sigma_{CF_2}l$ and an intercept of $1/OD_{max}$, where k_7 is the second-order rate constant. A representative plot at 249 nm for a C_2F_4 plus N_2 mixture is shown in Fig. 2. Similar plots were observed at 246 and 252 nm. These plots clearly demonstrated that CF_2 decay is second order. The slopes of the linear least-squares fits in all three cases were the same (within two standard deviations). The above wavelengths were chosen for detailed kinetic analyses, because the σ_{CF_2} values at these wavelengths are large (see Table 3); thus the CF_2 concentration could be monitored with reasonable accuracy up to 170 ms in most experiments. Decay kinetics in initial experiments were analyzed at the nine wavelengths identified earlier in Section 2 to establish unequivocally that the entire absorption spectra corresponded to one species, namely CF_2. By varying the flash energy between 50 and 288 J, different initial concentrations of CF_2

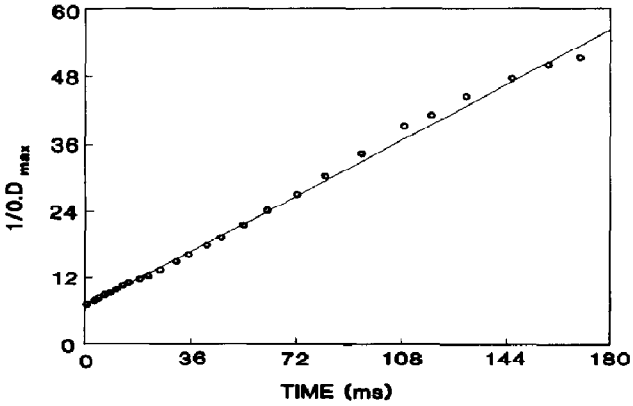

Fig. 2. Second-order decay plot for CF_2 in C_2F_4 photolysis at Λ = 249.0 nm ($P_{C_2F_4}$ = 10.1 Torr; P_{N_2} = 290.0 Torr; flash energy, 200 J; bandpass, 0.16 nm). The full line is the linear least-squares fit.

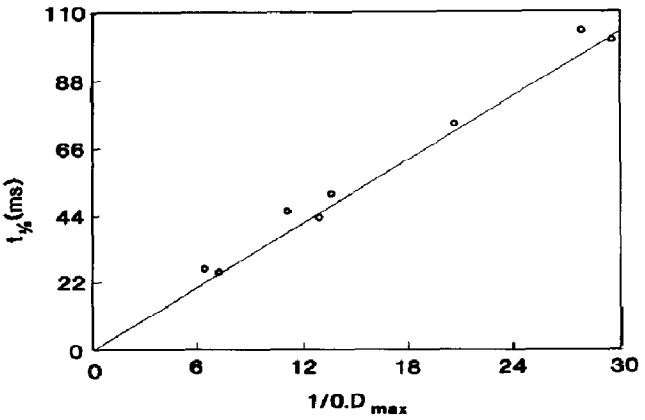

Fig. 3. Dependence of the half-life of CF_2 decay on $1/OD_{max}$ at Λ = 249.0 nm ($P_{C_2F_4}$ = 10.1 Torr; P_{N_2} = 290.0 Torr; bandpass, 0.16 nm; flash energies, between 50 and 288 J). The full line is a linear least-squares fit with a forced fit at the intercept of 0.0.

were produced. The variation in the half-life $t_{1/2}$ of CF_2 decay with $1/OD_{max}$ for a given mixture is shown in Fig. 3. Each point on this plot was determined by the photolysis of a fresh mixture. Figure 3 confirms that CF_2 follows a second-order decay. By plotting $2k_7/\sigma_{CF_2}l$, *i.e.* the slope from figures such as Fig. 2, against the pressure of the added gas, we were able to demonstrate that no complications from surface diffusion and three-body reactions existed in our experiments. An example of such results for M ≡ N_2 at 249.0 nm is shown in Fig. 4. Therefore, reaction (7), the second-order recombination of CF_2, is the only decay process important in our experiments on C_2F_4 photolysis.

On the basis of the above results on C_2F_4 experiments, we may expect that in the case of C_3F_6 photolysis also third-order recombination may not be important. This was confirmed for M ≡ N_2, M ≡ Ar and M ≡ SF_6 and is in agreement with the findings of Dalby [18] and Simons and Yarwood [22].

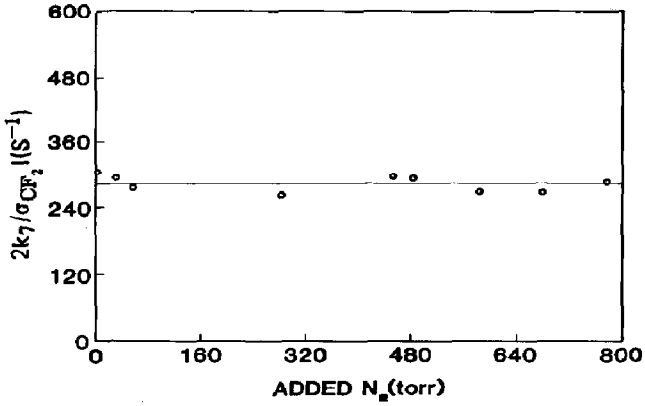

Fig. 4. $2k_7/\sigma_{CF_2}l$ *vs.* pressure of added N_2 at Λ = 249.0 nm for $P_{C_2F_4}$ = 10.0 - 10.35 Torr (flash energy, 200 J; bandpass, 0.16 nm).

Thus the two second-order recombination reactions for CF_2 in the photolysis of C_3F_6 are

$$CF_2 + CF_2 \longrightarrow C_2F_4 \quad (7)$$

$$CF_2 + C_3F_6 \longrightarrow C_4F_8 \quad (11)$$

By product analysis from multiflashed mixtures of C_3F_6 plus added gas using mass spectrometry and gas chromatography, we determined that C_2F_4 was the only product. This means that reaction (11) does not contribute appreciably to CF_2 decay. Figure 5 shows a second-order plot for C_3F_6 photolysis at 249.0 nm. Similar plots were observed at 246 and 252 nm. The results of all the experiments on C_3F_6 give $k_7 = (4.12 \pm 0.62) \times 10^{-14}$ cm^3 molecule^{-1} s^{-1}. Similarly, C_2F_4 experiments lead to a value of $k_7 = (4.33 \pm 0.58) \times 10^{-14}$ cm^3 molecule^{-1} s^{-1}. Therefore, on the basis of these identical values of k_7 and the analysis of photolysis products, we conclude that reaction (7) in both cases is the only recombination process important in the photolysis of both compounds. If we combine the k_7 values from all the experiments, C_2F_4, C_2F_4 plus added gas, C_3F_6 and C_3F_6 plus added gas, at the three wavelengths for which we have data on a large number of experiments, we obtain $k_7 = (4.26 \pm 0.64) \times 10^{-14}$ cm^3 molecule^{-1} s^{-1} at 298 ± 3 K. The ±15% quoted error is two standard deviations. This can be compared with the measurements of k_7 by Tyerman [17] from C_2F_4 photolysis and Dalby [18] who used C_3F_6 as a source for CF_2. The k_7 estimates at 298 K from their rate equations are $(3.66 \pm 0.73) \times 10^{-14}$ cm^3 molecule^{-1} s^{-1} and $(1.41 \pm 1.06) \times 10^{-14}$ cm^3 molecule^{-1} s^{-1} respectively. The disagreement with Dalby [18] may be due to the unaccounted variation of σ_{CF_2} with temperature as suggested by Tyerman [17]. It is interesting to note that in a study on IRMPD of CF_2HCl, Martinez *et al.* [4] find that computer modeling calculations lead to $k_7 = 3.65 \times 10^{-14}$ cm^3 molecule^{-1} s^{-1}. Statistically, our value of k_7 is indistinguishable from Tyerman's estimate [17]. However, we believe that our results represent an improvement in k_7 since the greater sensitivity

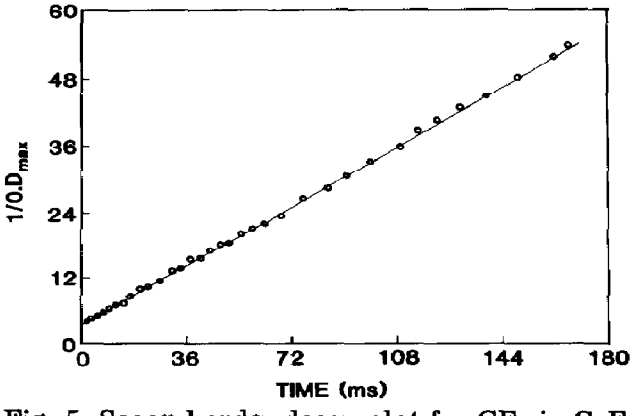

Fig. 5. Second-order decay plot for CF_2 in C_3F_6 photolysis at Λ = 249.0 nm ($P_{C_3F_6}$ = 20.1 Torr; P_{N_2} = 280.0 Torr; flash energy, 200 J; bandpass, 0.16 nm).

in our experiments allowed us to monitor kinetics well over three half-lives of CF_2 unlike in Tyerman's work where kinetic data on CF_2 decay appear to have been limited to a little over one half-life.

4. Conclusions

Absorption spectra of CF_2 at moderate dispersion where rotational structure at the band center remains unresolved were obtained by using C_2F_4 and C_3F_6 as sources of CF_2. The results are presented in the form of a table of σ_{CF_2} *vs.* wavelength at 0.5 nm intervals in the $\tilde{A}\ ^1B_1$–$\tilde{X}\ ^1A_1$ band from 229.0 to 262.5 nm.

The importance of reaction (4) as the dominant photodissociation channel in C_3F_6 photolysis was established. It was determined that CF_2 dimerizes by second-order kinetics and that CF_2 does not react with C_2F_4 or C_3F_6 to form the next higher perfluoroalkene.

The room temperature rate constant for reaction (7) was evaluated from a large number of experiments over a 25-fold variation in the initial concentration of CF_2.

Acknowledgments

Acknowledgment is made to the donors of the Petroleum Research Fund, administered by the American Chemical Society for partial support (PRF/ACS Grant 10117-B5,6) of this work during early stages. The authors express their sincere appreciation to Mr. Ron Nemeth for his generous help in the development of software for data acquisition. One of us (H.S.S.) would like to thank the Connecticut Technology Institute for summer support to gain a meaningful experience in real laboratory work while a junior at High School.

References

1 T. L. Burks and M. C. Lin, *J. Chem. Phys.*, *64* (1976) 4235.
2 R. R. Rebbert and P. J. Ausloos, *J. Photochem.*, *4* (1975) 419.
3 R. Duperrex and H. Van den Bergh, *J. Chem. Phys.*, *71* (1979) 3613.
4 R. I. Martinez, R. E. Huie, J. T. Herron and W. Braun, *J. Phys. Chem.*, *84* (1980) 2344.
5 G. R. Long, L. D. Prentice and S. E. Bialkowski, *Appl. Phys. B*, *34* (1984) 34.
6 W. S. Nip, M. Drouin, P. A. Hackett and C. Willis, *J. Phys..Chem.*, *84* (1980) 932.
7 D. M. Rayner, S. Kimel and P. A. Hackett, *Chem. Phys. Lett.*, *96* (1983) 678.
8 J. J. Tiee, F. B. Wampler and W. W. Rice, *Chem. Phys. Lett.*, *68* (1979) 403.
9 C. R. Moylan and J. I. Brauman, *Int. J. Chem. Kinet.*, *18* (1986) 379.
10 J. R. Gilbert, I. R. Slagle, R. E. Graham and D. Gutman, *J. Phys. Chem.*, *80* (1976) 14.
11 P. J. Hargis and M. J. Kushner, *Appl. Phys. Lett.*, *40* (1982) 779.

12 S. Koda, *Chem. Phys. Lett.*, *55* (1978) 353.
13 S. Koda, *J. Phys. Chem.*, *83* (1979) 2065.
14 G. O. Pritchard, K. A. Johnson and W. B. Nilsson, *Int. J. Chem. Kinet.*, *17* (1985) 327.
15 S. W. Benson, *Adv. Photochem.*, *2* (1964) 1.
16 G. O. Pritchard, W. B. Nilsson and B. Kirtman, *Int. J. Chem. Kinet.*, *16* (1984) 1637.
17 W. J. R. Tyerman, *Trans. Faraday Soc.*, *64* (1969) 1188.
18 F. W. Dalby, *J. Chem. Phys.*, *41* (1964) 2297.
19 C. Weldon Mathews, *Can. J. Phys.*, *45* (1967) 2355.
20 H. Okabe, *Photochemistry of Small Molecules*, Wiley-Interscience, New York, 1978, p. 125.
21 D. S. King, P. K. Schenck and J. C. Stephenson, *J. Mol. Spectrosc.*, *78* (1979) 1.
22 J. P. Simons and A. J. Yarwood, *Nature (London)*, *187* (1960) 316.